EM-BASED SPARSE IMAGING FOR COLOCATED MIMO RADAR UNDER PHASE SYNCHRONIZATION MISMATCH

Li Ding, Weidong Chen, Wenyi Zhang

Department of Electronic Engineering and Information Science
University of Science and Technology of China, Hefei, Anhui, P.R. China
Email: lilyding@mail.ustc.edu.cn, {wdchen, wenyizha}@ustc.edu.cn

ABSTRACT

Multiple-input multiple-output (MIMO) radar with colocated antennas is expected to achieve good imaging performance via coherent processing. However, a crucial factor to this process−phase synchronization, which directly determines the performance gain, has rarely been studied in previous works. Hence in this paper, given the sparsity of the target, we address the problem of imaging for colocated MIMO radar under the phase synchronization mismatch. Based on the model assumption that the phase synchronization mismatch in each propagation path is an independent and identically distributed uniform random variable, we combine the sparsity of the target and expectation maximization (EM) method to develop an EM-based sparse imaging algorithm against such random phase mismatch. The effectiveness of the proposed algorithm is demonstrated by numerical simulations.

***Index Terms*—** Expectation maximization, MIMO radar, phase synchronization mismatch, sparse imaging

1. INTRODUCTION

Together with the sparse priority of target, Multiple-input-multiple-output (MIMO) radar with colocated antennas has been shown to be of great ability to provide high-resolution imaging in the wavenumber domain [1] [2] [3].

This good reconstruction performance is mainly brought by coherent processing. However, the phase synchronization− a crucial factor to coherent processing− is hard to realize perfectly and thus always an inevitable problem. Its imperfect implementation evidently could lead to performance degradation. As to phase synchronization mismatch in MIMO radar, its influence on detection has been studied in [4], on localization in [5][6], and further on tracking in [7], but relatively less attention has been paid on colocated MIMO radar imaging. Hence, under the premise of sparse target, we investigate the problem of colocated MIMO radar imaging associated with random phase synchronization mismatch. In this case, the reconstruction is not straightforward because of the randomness of phase mismatch, and the conventional sparse recovery techniques [8], such as the Lasso algorithm, would become inefficient. So we resort to the combination of expectation maximization (EM) method [9] and sparsity of target to develop an EM-based sparse imaging algorithm. In addition to the sparse priority, our algorithm also takes advantage of EM method to efficiently exploit the statistical property of signal and provides high reconstruction performance by iteratively alternating between the expectation stage and maximization stage.

Notations: $(\cdot)^*$, $(\cdot)^T$ and $(\cdot)^H$ denote the conjugate, the transpose and the conjugate transpose operation respectively. diag$(\cdot)$ indicates diagonalization while blkdiag$(\cdot)$ is the block diagonalization. $\sinh(\cdot)$, $\cosh(\cdot)$ and $\coth(\cdot)$ mean the hyperbolic sin, the hyperbolic cosine and the hyperbolic cotangent function, respectively.

The work in this paper is supported by National Natural Science Foundation of China under Grant No. 61172155.

2. SIGNAL MODEL

Consider a two dimensional (2-D) colocated MIMO radar with M transmitters and N receivers in wavenumber domain [1] . Define (R_m^{Tx}, ϕ_m^{Tx}) (for $m = 1, \cdots, M$) and (R_n^{Rx}, ϕ_n^{Rx}) (for $n = 1, \cdots, N$) as the positions in the polar coordinate of the m-th transmitter and the n receiver, respectively. The center of imaging scene of interest is regarded as the origin of the coordinate and we suppose that there are only L scatterers. Exploiting the far-field approximation and orthogonality separation, we can obtain the echo with the phase synchronization mismatch ψ_{nm} at the n-th receiver corresponding to the m-th transmitter as

$$y_{nm}(f) = \sum_{l=1}^{L} \sigma(\mathbf{r}_l)\, \mathrm{e}^{\mathrm{j}2\pi \mathbf{K}_{nm}(f)\cdot \mathbf{r}_l} \mathrm{e}^{-\mathrm{j}\psi_{nm}} + z_{nm}(f) \quad (1)$$

where $\sigma(\mathbf{r}_l)$ denotes the complex reflectivity of the l-th scatterer with the location $\mathbf{r}_l = (x_l, y_l)$ (for $l = 1, \cdots, L$). $z_{nm}(f)$ is the additive noise. $\mathbf{K}_{nm}(f)$ indicates the sampling of 2-D wavenumber domain, given as (K_{nm}^x, K_{nm}^y),

$$\begin{cases} K_{nm}^x(f) = \frac{f+f_m}{\mathrm{c}} \left(\cos\phi_m^{Tx} + \cos\phi_n^{Rx}\right) \\ K_{nm}^y(f) = \frac{f+f_m}{\mathrm{c}} \left(\sin\phi_m^{Tx} + \sin\phi_n^{Rx}\right) \end{cases} \quad (2)$$

where $f \in [-\frac{B_m}{2}, \frac{B_m}{2}]$, B_m and f_m are the narrow bandwidth and the carrier frequency of the m-th transmitted signal, respectively. c is the propagation velocity of electromagnetic wave. A compact form of (1) can be written as

$$y_{nm}(f) = \mathrm{e}^{-\mathrm{j}\psi_{nm}} \mathbf{a}_{nm}^T(f)\,\boldsymbol{\sigma} + z_{nm}(f) \tag{3}$$

where $\boldsymbol{\sigma} = [\sigma(\mathbf{r}_1) \cdots \sigma(\mathbf{r}_L)]^T$, $\mathbf{a}_{nm}(f)$ is an $L \times 1$ vector and its l-th element has the form of $\mathrm{e}^{\mathrm{j}2\pi \mathbf{K}_{nm}(f)\cdot \mathbf{r}_l}$. We assume that there are K frequency sampling points and stack them into a $K \times 1$ vector, $\mathbf{y}_{nm} = [y_{nm}(f_1), \cdots, y_{nm}(f_K))]^T$, i.e.,

$$\mathbf{y}_{nm} = \boldsymbol{\Psi}_{nm}\mathbf{A}_{nm}\boldsymbol{\sigma} + \mathbf{z}_{nm} \tag{4}$$

where $\boldsymbol{\Psi}_{nm} = \mathrm{diag}\left(\mathrm{e}^{-\mathrm{j}\psi_{nm}(1)}, \cdots \mathrm{e}^{-\mathrm{j}\psi_{nm}(K)}\right)$ and is the sampling matrix of phase error corresponding to the nm-th propagation path which refers to the path from the m-th transmitter to the n-th receiver. $\mathbf{A}_{nm} = [\mathbf{a}_{nm}(f_1), \cdots, \mathbf{a}_{nm}(f_K)]^T$ and $\mathbf{z}_{nm} = [z_{nm}(f_1), \cdots, z_{nm}(f_K)]^T$. Then, combining all the observations from NM propagation paths, we obtain

$$\mathbf{y} = [{\mathbf{y}_{11}}^T, \cdots, {\mathbf{y}_{NM}}^T]^T = \boldsymbol{\Psi}\mathbf{A}\boldsymbol{\sigma} + \mathbf{z} \tag{5}$$

where $\mathbf{z} = [\mathbf{z}_{11}^T, \cdots, \mathbf{z}_{NM}^T]^T$, $\mathbf{A} = [\mathbf{A}_{11}^T, \cdots \mathbf{A}_{NM}^T]^T$, and $\boldsymbol{\Psi} = \mathrm{blkdiag}\left(\boldsymbol{\Psi}_{11}, \cdots, \boldsymbol{\Psi}_{NM}\right)$.

In (5), we assume $\mathbf{z}$ is independent and identically distributed (i.i.d.) zero-mean complex multivariate normal random vector with unknown covariance matrix $\eta\mathbf{I}$ ($\mathbf{I}$ is a $NMK \times NMK$ unit matrix) and assume all the $\psi_{nm}(k)$ being i.i.d. and obeying uniform distribution over the relatively small range $[-\Delta\pi, \Delta\pi]$ ($|\Delta| < \zeta$, ζ delineates the possibly maximal spread of the density). For simplicity, let $\rho = NMK$ and $\boldsymbol{\Theta}$ be the collection set of $\{\psi_{nm}(k)\}$ for $n = 1, \cdots, N$, $m = 1, \cdots, M$, $k = 1, \cdots, K$. Hence, conditioned on $\boldsymbol{\Theta}$ with known $\mathbf{A}$ and unknown $\boldsymbol{\sigma}$, Δ and η, we get the following probability distribution for (5)

$$p\left(\mathbf{y}\,|\Delta, \eta, \boldsymbol{\Theta}, \boldsymbol{\sigma}\right) = \tfrac{1}{(\pi\eta)^{\rho}} \mathrm{e}^{-\frac{1}{\eta}\|\mathbf{y} - \boldsymbol{\Psi}\mathbf{A}\boldsymbol{\sigma}\|_2^2}\,. \tag{6}$$

Given the statistical assumption above, the solutions for maximum likelihood estimates of $\boldsymbol{\sigma}, \eta, \Delta$ from the observed data likelihood function $p\left(\boldsymbol{\sigma}, \eta, \Delta\,|\mathbf{y}\right)$ is not straightforward. Therefore, we resort to EM method; cf. [4]. Define $(\mathbf{y}, \boldsymbol{\Theta})$ and $(\Delta, \eta, \boldsymbol{\sigma})$ as the complete data and parameter sets, denoted as $\boldsymbol{\gamma}_{cd}$ and $\boldsymbol{\Lambda}$, respectively. The jointly probability function for $\boldsymbol{\gamma}_{cd}$ and $\boldsymbol{\Lambda}$ is computed as (7) based on the independency among $\boldsymbol{\sigma}, \eta$ and $\{\boldsymbol{\Theta}, \Delta\}$

$$p\left(\boldsymbol{\gamma}_{cd}, \boldsymbol{\Lambda}\right) = p\left(\boldsymbol{\sigma}\right) p\left(\eta\right) p\left(\boldsymbol{\Theta}, \Delta\right) p\left(\mathbf{y}\,|\eta, \boldsymbol{\Theta}, \boldsymbol{\sigma}, \Delta\right) \tag{7}$$

where $p\left(\eta\right) = p\left(\boldsymbol{\sigma}\right) = 1$ (for the consideration of their deterministic characteristic), and $p\left(\boldsymbol{\Theta}, \Delta\right)$ takes the form as

$$\prod_{n=1}^{N}\prod_{m=1}^{M}\prod_{k=1}^{K} p(\psi_{nm}(k), \Delta) = \prod_{n=1}^{N}\prod_{m=1}^{M}\prod_{k=1}^{K} \frac{1}{2\Delta\pi}. \tag{8}$$

Subtituting (6) and (8) into (7), we get its log-likelihood function in a unfolded expression as

$$\begin{aligned}\ln p(\boldsymbol{\gamma}_{cd}, \boldsymbol{\Lambda}) = \mathrm{C} &- \rho\ln\eta - \rho\ln\Delta \\ &-\frac{1}{\eta}\left(\|\mathbf{y}\|_2^2 + \boldsymbol{\sigma}^H\mathbf{A}^H\mathbf{A}\boldsymbol{\sigma}\right) \\ &+\frac{2}{\eta}\,\mathrm{Re}\left\{\mathbf{y}^H\boldsymbol{\Psi}\mathbf{A}\boldsymbol{\sigma}\right\}\end{aligned} \tag{9}$$

where C is a constant. If there is no phase synchronization mismatch, i.e., $\boldsymbol{\Psi} = \mathbf{I}$, the estimation of the parameter set would degenerate into a problem to maximize $\ln p(\boldsymbol{\gamma}_{cd}, \boldsymbol{\Lambda})$ with respect to $\boldsymbol{\Lambda}$. Specifically, under the sparsity of the target in terms of l_1-norm, the popular sparse imaging would be implemented by minimizing $\lambda\|\boldsymbol{\sigma}\|_1 + \|\mathbf{y} - \mathbf{A}\boldsymbol{\sigma}\|_2^2$ (λ is a penalty factor), i.e, the Lasso algorithm [8] which will then be used as a baseline in Section 4.

3. EM-BASED SPARSE IMAGING

Due to the existence of mismatch matrix $\boldsymbol{\Psi}$, the performance degradation by conventional sparse imaging is inevitable. Therefore, the EM method which efficiently exploits the statistical property of signal model and does increase the likelihood function with the growth of iteration is used. Our EM-based sparse imaging consisting of two stages−expectation (**E**-stage) and maximization (**M**-stage)−is detailed below.

3.1. E-stage

In the **E**-stage of the q-th iteration, we compute the conditional expectation of (9) given the observed data $\mathbf{y}$ and the estimated parameter set $\boldsymbol{\Lambda}^{(q-1)}$ (i.e. $\boldsymbol{\Lambda}^{(q-1)} = \{\Delta^{(q-1)}, \eta^{(q-1)}, \boldsymbol{\sigma}^{(q-1)}\}$) which is attained in the former **M**-stage of the $(q-1)$-th iteration, as shown in (10)

$$\begin{aligned} &L_{cd}\left(\boldsymbol{\Lambda}^{(q-1)}\right) = E_{p(\boldsymbol{\Theta}|\mathbf{y})}\left\{\ln p(\boldsymbol{\gamma}_{cd}, \boldsymbol{\Lambda})\,\middle|\mathbf{y}, \boldsymbol{\Lambda}^{(q-1)}\right\} \\ &= -\rho\ln\eta^{(q-1)} - \rho\ln\Delta^{(q-1)} \\ &\quad -\frac{1}{\eta^{(q-1)}}\left(\|\mathbf{y}\|_2^2 + \left(\boldsymbol{\sigma}^{(q-1)}\right)^H\mathbf{A}^H\mathbf{A}\boldsymbol{\sigma}^{(q-1)}\right) \\ &\quad +\frac{2}{\eta^{(q-1)}}\,\mathrm{Re}\left\{E_{p(\boldsymbol{\Theta}|\mathbf{y})}\left\{\mathbf{y}^H\boldsymbol{\Psi}\mathbf{A}\boldsymbol{\sigma}|\mathbf{y}, \boldsymbol{\Lambda}^{(q-1)}\right\}\right\}\end{aligned} \tag{10}$$

where the constant term has been suppressed. We can compute the conditional distribution $p(\boldsymbol{\Theta}|\mathbf{y})$ through $p(\boldsymbol{\Theta}, \mathbf{y})$ and $p(\mathbf{y})$, where

$$\begin{aligned} p\left(\boldsymbol{\Theta}, \mathbf{y}\right) &= \frac{1}{(\pi\eta)^{\rho}}\mathrm{e}^{-\frac{1}{\eta}\|\mathbf{y} - \boldsymbol{\Psi}\mathbf{A}\boldsymbol{\sigma}\|_2^2}\left(\frac{1}{2\pi\Delta}\right)^{\rho} \\ p\left(\mathbf{y}\right) &= \int_{-\Delta\pi}^{\Delta\pi}\cdots\int_{-\Delta\pi}^{\Delta\pi} p\left(\boldsymbol{\Theta}, \mathbf{y}\right) d\boldsymbol{\Theta}\end{aligned}\,. \tag{11}$$

Additionally, $\psi_{nm}(k)$ is assumed to vary in a relatively small range so that such approximations, i.e., $\sin(\psi_{nm}(k)) \approx \psi_{nm}(k)$ and $\cos(\psi_{nm}(k)) \approx 1$, are roughly available, then $p(\boldsymbol{\Theta}|\mathbf{y})$ can be computed as

$$p\left(\boldsymbol{\Theta}\,|\mathbf{y}\right) = \prod_{n=1}^{N}\prod_{m=1}^{M}\prod_{k=1}^{K}\frac{v_{nm}^k\left(\boldsymbol{\sigma}\right)\mathrm{e}^{\frac{2}{\eta}v_{\mathrm{nm}}^{\mathrm{k}}(\boldsymbol{\sigma})\psi_{\mathrm{nm}}(\mathrm{k})}}{\eta\sinh\left(\frac{2\Delta\pi}{\eta}v_{nm}^k\left(\boldsymbol{\sigma}\right)\right)} \tag{12}$$

where $v_{nm}^k\left(\boldsymbol{\sigma}\right) = \mathrm{Im}\left\{y_{nm}^*\left(f_k\right)\mathbf{a}_{nm}^T\left(f_k\right)\boldsymbol{\sigma}\right\}$.

Hence, the last term of the right side of the second equation in (10) could be approximated as

$$\begin{aligned}&\mathrm{Re}\left\{\frac{2}{\eta^{(q-1)}}E_{p(\boldsymbol{\Theta}|\mathbf{y})}\left\{\mathbf{y}^H\boldsymbol{\Psi}\mathbf{A}\boldsymbol{\sigma}|\mathbf{y},\boldsymbol{\Lambda}^{(q-1)}\right\}\right\}\\&\approx\frac{2\mathrm{Re}\left\{\mathbf{y}^H\mathbf{A}\boldsymbol{\sigma}^{(q-1)}\right\}}{\eta^{(q-1)}}+\sum_{n=1}^{N}\sum_{m=1}^{M}\sum_{k=1}^{K}h_{nm}^k(\boldsymbol{\Lambda}^{(q-1)})\end{aligned}\tag{13}$$

where $h_{nm}^k(\boldsymbol{\Lambda}^{(q-1)})=\frac{2}{\eta^{(q-1)}}E_{p(\boldsymbol{\Theta}|\mathbf{y})}\left\{v_{nm}^k(\boldsymbol{\sigma})\psi_{nm}(k)|\mathbf{y},\boldsymbol{\Lambda}^{(q-1)}\right\}$. This conditional expectation can be derived through (12), and omitting the subscript $(q-1)$, we have

$$h_{nm}^k(\boldsymbol{\Lambda})=\left(\frac{2\Delta\pi}{\eta}v_{nm}^k(\boldsymbol{\sigma})\right)\coth(\frac{2\Delta\pi}{\eta}v_{nm}^k(\boldsymbol{\sigma}))-1.\tag{14}$$

3.2. M-stage

Since the conditional expectation $L_{cd}(\boldsymbol{\Lambda})$ in (10) through **E**-stage is a function of the parameter set $\boldsymbol{\Lambda}$, it is natural to maximize (10) with respect to $\boldsymbol{\Lambda}$, i.e. $\max_{\boldsymbol{\Lambda}} L_{cd}(\boldsymbol{\Lambda}) = \max_{\eta}\max_{\Delta}\max_{\boldsymbol{\sigma}} L_{cd}(\boldsymbol{\Lambda})$, to get their MLEs in the **M**-stage at the q-th iteration.

For $\boldsymbol{\sigma}$, the equivalent problem of sparse reconstruction is identical to solve

$$\min_{\boldsymbol{\sigma}}\left\{\begin{aligned}&\lambda\|\boldsymbol{\sigma}\|_1+\frac{1}{\eta^{(q-1)}}\boldsymbol{\sigma}^H\mathbf{A}^H\mathbf{A}\boldsymbol{\sigma}-\frac{2}{\eta^{(q-1)}}\mathrm{Re}\left\{\mathbf{y}^H\mathbf{A}\boldsymbol{\sigma}\right\}\\&-\sum_{n=1}^{N}\sum_{m=1}^{M}\sum_{k=1}^{K}h_{nm}^k\left(\Delta^{(q-1)},\eta^{(q-1)},\boldsymbol{\sigma}\right)\end{aligned}\right\}.\tag{15}$$

Due to the non-convex character of $\coth(\cdot)$ coming from the conditional expectation, the conventional methods for convex optimization will not be appropriate here. However, this function is differentiable apart from the origin point and Newton-Raphson method is specialized to find stationary points of differentiable functions [10]. Herein, we exploit Newton-Raphson method to seek for the solution of $\boldsymbol{\sigma}$ at the current iteration. Let $f(\boldsymbol{\Lambda})$ substitute the objective function in (15), and then, its first-order derivative is

$$\begin{aligned}\nabla_{\boldsymbol{\sigma}^*}f(\boldsymbol{\Lambda})&=\nabla_{\boldsymbol{\sigma}^*}(\lambda\|\boldsymbol{\sigma}\|_1)+\frac{2}{\eta}\mathbf{A}^H\mathbf{A}\boldsymbol{\sigma}-\frac{2}{\eta}\mathbf{A}^H\mathbf{y}\\&-\sum_{n=1}^{N}\sum_{m=1}^{M}\sum_{k=1}^{K}\frac{\partial h_{nm}^k(\boldsymbol{\Lambda})}{\partial v_{nm}^k(\boldsymbol{\sigma})}\frac{\partial v_{nm}^k(\boldsymbol{\sigma})}{\partial\boldsymbol{\sigma}^*}\end{aligned}\tag{16}$$

where

$$\begin{aligned}\frac{\partial h_{nm}^k(\boldsymbol{\Lambda})}{\partial v_{nm}^k(\boldsymbol{\sigma})}&=\frac{h_{nm}^k(\boldsymbol{\Lambda})+1}{v_{nm}^k(\boldsymbol{\sigma})}\left(1-\frac{h_{nm}^k(\boldsymbol{\Lambda})+1}{\cosh^2(\frac{2\Delta\pi}{\eta}v_{nm}^k(\boldsymbol{\sigma}))}\right).\\\frac{\partial v_{nm}^k(\boldsymbol{\sigma})}{\partial\boldsymbol{\sigma}^*}&=\frac{j}{2}y_{nm}(f_k)\,\mathbf{a}_{nm}^*(f_k)\end{aligned}\tag{17}$$

Then the Hessian matrix of $f(\boldsymbol{\Lambda})$ is

$$\begin{aligned}\nabla_{\boldsymbol{\sigma}}^2 f(\boldsymbol{\Lambda})&=\nabla_{\boldsymbol{\sigma}}^2(\lambda\|\boldsymbol{\sigma}\|_1)+\frac{2}{\eta}\mathbf{A}^H\mathbf{A}\\&-\sum_{n=1}^{N}\sum_{m=1}^{M}\sum_{k=1}^{K}g_{nm}^k(\boldsymbol{\Lambda})\frac{\partial v_{nm}^k(\boldsymbol{\sigma})}{\partial\boldsymbol{\sigma}^*}\frac{\partial v_{nm}^k(\boldsymbol{\sigma})}{\partial\boldsymbol{\sigma}^T}\end{aligned}\tag{18}$$

where

$$\begin{aligned}g_{nm}^k(\boldsymbol{\Lambda})&=\frac{2(h_{nm}^k(\boldsymbol{\Lambda})+1)^2h_{nm}^k(\boldsymbol{\Lambda})}{(v_{nm}^k(\boldsymbol{\sigma}))^2\cosh^2\left(\frac{2\Delta\pi}{\eta}v_{nm}^k(\boldsymbol{\sigma})\right)}.\\\frac{\partial v_{nm}^k(\boldsymbol{\sigma})}{\partial\boldsymbol{\sigma}^T}&=\frac{1}{2j}y_{nm}^*(f_k)\,\mathbf{a}_{nm}^T(f_k)\end{aligned}\tag{19}$$

Hence, at the q-th iteration, a series of inner iterations, denoted as $\boldsymbol{\sigma}_{(i)}^{(q)}$ (for $i=1,2,\cdots$), is established to estimate the current $\boldsymbol{\sigma}^{(q)}$, in which the previously estimated $\boldsymbol{\sigma}^{(q-1)}$ is used as the initial value, i.e. $\boldsymbol{\sigma}_{(0)}^{(q)}$. This inner iteration is presented as

$$\boldsymbol{\sigma}_{(i)}^{(q)}=\boldsymbol{\sigma}_{(i-1)}^{(q)}-[\mathbf{H}_{(i)}^{(q)}]^{-1}\nabla_{\boldsymbol{\sigma}^*}f\left(\Delta^{(q-1)},\eta^{(q-1)},\boldsymbol{\sigma}_{(i)}^{(q)}\right)\tag{20}$$

where $\mathbf{H}_{(i)}^{(q)}=\nabla_{\boldsymbol{\sigma}}^2 f\left(\Delta^{(q-1)},\eta^{(q-1)},\boldsymbol{\sigma}_{(i-1)}^{(q)}\right)+\mathbf{B}_{(i)}^{(q)}$, and $\mathbf{B}_{(i)}^{(q)}$ is the digonal matrix to guarantee the invertibility of Hessain matrix, that is, $\mathbf{H}_{(i)}^{(q)}\geqslant\mathbf{0}$. The inner iteration yields $\boldsymbol{\sigma}^{(q)}$ when $\boldsymbol{\sigma}_{(i)}^{(q)}$ reaches its stationary point.

Similarly, the parameter Δ and η will be updated by maximizing $L_{cd}\left(\Delta,\eta^{(q-1)},\boldsymbol{\sigma}^{(q)}\right)$ and $L_{cd}\left(\Delta^{(q)},\eta,\boldsymbol{\sigma}^{(q)}\right)$ with respect to Δ and η, respectively. That means

$$\min_{\Delta}\left\{\rho\ln\Delta-\sum_{n=1}^{N}\sum_{m=1}^{M}\sum_{k=1}^{K}h_{nm}^k\left(\Delta,\eta^{(q-1)},\boldsymbol{\sigma}^{(q)}\right)\right\}.\tag{21}$$

$$\min_{\eta}\left\{\begin{aligned}&\rho\ln\eta+\frac{1}{\eta}\left(\|\mathbf{y}\|_2^2+\left(\boldsymbol{\sigma}^{(q)}\right)^H\mathbf{A}^H\mathbf{A}\boldsymbol{\sigma}^{(q)}\right)\\&-\frac{1}{\eta}\mathrm{Re}\left\{E_{p(\boldsymbol{\Theta}|\mathbf{y})}\left\{\mathbf{y}^H\boldsymbol{\Psi}\mathbf{A}\boldsymbol{\sigma}\,\Big|\mathbf{y},\Delta^{(q)},\boldsymbol{\sigma}^{(q)}\right\}\right\}\end{aligned}\right\}.\tag{22}$$

Also, Newton-Raphson method is utilized in (21) and (22) to obtain $\Delta^{(q)}$ and $\eta^{(q)}$.

The **E**-stage and **M**-stage alternatively iterate until $\boldsymbol{\sigma}^{(q)}$, $\Delta^{(q)}$ and $\eta^{(q)}$ converge.

4. SIMULATION

We consider a 2-D colocated MIMO radar with $M=N=5$. The transmitters and receivers are uniformly distributed, and

Table 1. Parameters of MIMO radar

Carrier frequency	f_0	8.9GHz
Narrow bandwidth	B_m	50MHz
Transmitter Position	(x_m^{Tx},y_m^{Tx})	(-10Km, $25(m-1)$m)
Receiver Position	(x_n^{Rx},y_n^{Rx})	(-10Km, $5(n-1)$m)

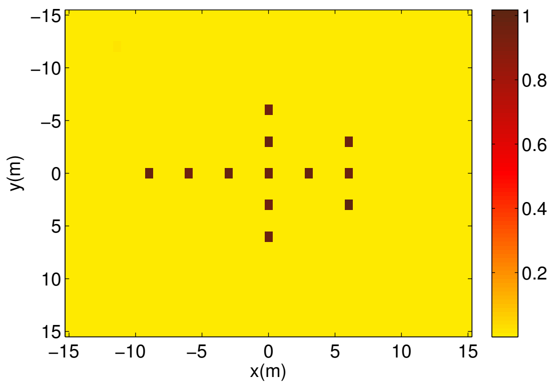

(a) absence of phase synchronization mismatch

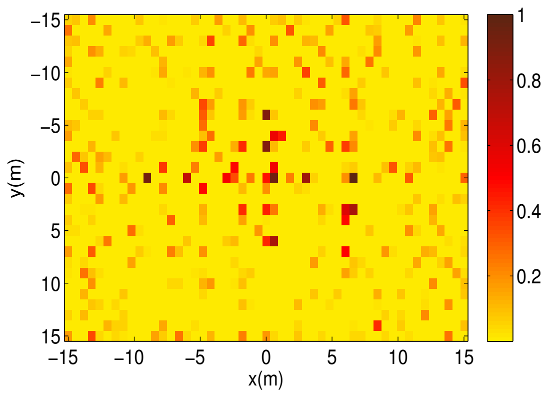

(b) presence of phase synchronization mismatch

Fig. 1. Imaging by minimizing $\lambda \|\boldsymbol{\sigma}\|_1 + \|\mathbf{y} - \mathbf{A}\boldsymbol{\sigma}\|_2^2$

their positions are expressed in the Cartesian coordinate, that is, $(x_m^{Tx}, y_m^{Tx}) = R_m^{Tx}(\cos\phi_m^{Tx}, \sin\phi_m^{Tx})$ and $(x_n^{Rx}, y_n^{Rx}) = R_n^{Rx}(\cos\phi_n^{Rx}, \sin\phi_n^{Rx})$. The carrier frequency of the m-th transmitted signal is $f_m = f_0 + (m-1)B_m$ and f_0 corresponds to the first transmitter. The detail parameters are shown in Table 1. Moreover, λ equals 1, the signal-to-noise ratio is set to 10dB and Δ takes the value of $1/6$.

From the comparasion between Fig.1(a) and Fig.1(b), it is obvious that in the presence of phase mismatch, the imaging performance by minimizing $\lambda \|\boldsymbol{\sigma}\|_1 + \|\mathbf{y} - \mathbf{A}\boldsymbol{\sigma}\|_2^2$ is seriously degraded.

Fig.2 shows that the proposed EM-based algorithm which takes the result of Fig.1(b) as the initial value $\boldsymbol{\sigma}^{(0)}$ remarkably improves the negative impact affected due to phase synchronization mismtch.

5. CONCLUSION

For the sparse imaging in colocated MIMO radar, we present an EM-based sparse imaging algorithm to realize reconstruction under the phase synchronization mismatch. This proposed algorithm efficiently exploits the statistical property of phase mismatch. In spite of the trigonometric function approximation in (12), it wouldn't restrict our algorithm to merely face up a relatively small spread of phase synchronization error. The simulations clearly confirm this advantage of our algorithm, as well as its competence to support better reconstruction performance.

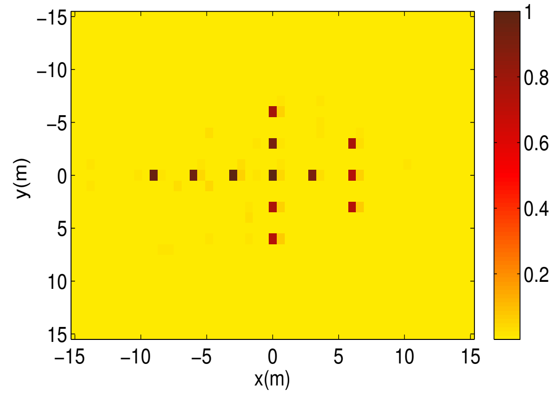

Fig. 2. Imaging by the EM-based algorithm

6. REFERENCES

[1] X. Hao, H. Xuezhi, Y. Zhiping, W. Dongjin, and C. Weidong, "Compressive sensing mimo radar imaging based on inverse scattering model," in *Signal Processing (ICSP), 2010 IEEE 10th International Conference on*. IEEE, 2010, pp. 1999–2002.

[2] X. Tan, W. Roberts, J. Li, and P. Stoica, "Sparse learning via iterative minimization with application to mimo radar imaging," *Signal Processing, IEEE Transactions on*, vol. 59, no. 3, pp. 1088–1101, 2011.

[3] X. Zhuge and A. G. Yarovoy, "A sparse aperture mimo-sar-based uwb imaging system for concealed weapon detection," *Geoscience and Remote Sensing, IEEE Transactions on*, vol. 49, no. 1, pp. 509–518, 2011.

[4] M. Akçakaya and A. Nehorai, "Mimo radar detection and adaptive design under a phase synchronization mismatch," *Signal Processing, IEEE Transactions on*, vol. 58, no. 10, pp. 4994–5005, 2010.

[5] H. Godrich and A. Haimovich, "Localization performance of coherent mimo radar systems subject to phase synchronization errors," in *Communications, Control and Signal Processing (ISCCSP), 2010 4th International Symposium on*. IEEE, 2010, pp. 1–5.

[6] A. Haimovich, "Distributed mimo radar for imaging and high resolution target localization," DTIC Document, Tech. Rep., 2012.

[7] P. Ma, Q. Zhou, and J. Zhang, "Antenna placement analysis for coherent mimo radar with phased synchronization errors," *Applied Mechanics and Materials*, vol. 121, pp. 3689–3693, 2012.

[8] T. Strohmer and B. Friedlander, "Compressed sensing for mimo radar-algorithms and performance," in *Signals, Systems and Computers, 2009 Conference Record of the Forty-Third Asilomar Conference on*. IEEE, 2009, pp. 464–468.

[9] A. Dempster, N. Laird, and D. Rubin, "Maximum likelihood from incomplete data via the em algorithm," *Journal of the Royal Statistical Society. Series B (Methodological)*, pp. 1–38, 1977.

[10] S. Boyd and L. Vandenberghe, *Convex optimization*. Cambridge university press, 2004.